

Cite this: *CrystEngComm*, 2014, **16**, 2959–2968

## A series of 2-D and 3-D silver(i) coordination polymers constructed from a new angular-shaped di-2-pyrazinylsulfide: role of anions in molecular construction<sup>†‡</sup>

Chong-Qing Wan,\* Ya Zhang, Xin-Zhan Sun and Hao-Jie Yan

Seven coordination polymers (CPs) based on a new multidentate di-2-pyrazinylsulfide (DpzS) ligand and various anions, namely  $\{[Ag_3(DpzS)_2(ClO_4)_2](ClO_4)_2\}_{\infty}$  (1),  $[Ag_3(DpzS)_2(CF_3SO_3)_3]_{\infty}$  (2),  $\{[Ag_3(DpzS)_2(CF_3SO_3)(H_2O)_2](CF_3SO_3)_2 \cdot H_2O\}_{\infty}$  (3),  $[Ag_2(DpzS)(NO_3)_2(H_2O)]_{\infty}$  (4),  $[Ag(DpzS)(NO_2)]_{\infty}$  (5),  $[Ag_2(DpzS)(NO_2)_2]_{\infty}$  (6) and  $[Ag_2(DpzS)(C_2F_5CO_2)_2]_{\infty}$  (7), have been synthesized and fully characterized by IR spectroscopy, elemental analyses, single crystal X-ray diffraction and powder X-ray diffraction. In 1–7, the DpzS ligand exhibits diverse coordination modes with various silver(i) salts, yielding fascinating 2-D and 3-D topological frameworks. The effect of the anion, such as the size and geometry, on the structural diversities of 1–7 has been discussed. In addition, the role played by anion–π(pyrazinyl) interaction in the supramolecular assembly of 1–7 has also been studied.

Received 25th November 2013,  
Accepted 20th January 2014

DOI: 10.1039/c3ce42404a

[www.rsc.org/crystengcomm](http://www.rsc.org/crystengcomm)

## Introduction

The design and synthesis of coordination polymers (CPs) has become a subject of extensive investigation because of their fascinating architectures and functional properties.<sup>1</sup> So far, various CPs with interesting structures and properties have been designed and assembled by careful selection of basic components, such as the coordination geometry of metal ions, the length of spacers, the binding site of donating atoms, and/or by the induction of weak intra- or intermolecular interactions.<sup>1</sup> In this regard, the organic ligands with functional groups play a major role in determining network geometries and properties. Angular-shaped ligands, such as semi-rigid di-2-pyrimidyl sulfide and its N-positional isomers exhibit more flexible ligation modes in the construction of diverse coordination motifs with unusual properties.<sup>2</sup> However, their analog, the new angular ligand di-2-pyrazinylsulfide (abbreviated as DpzS) (Scheme 1),

has received less attention in the construction of CPs.<sup>3</sup> The angular DpzS ligand is a good candidate for the assembly of CPs.<sup>4</sup> The DpzS ligand contains a pair of pyrazinyl rings lying on two sides of the central sulfur atom, wherein one or both nitrogen ligation site(s) on each heteroaromatic ring may exhibit diverse coordination modes to generate various supramolecular networks. Moreover, the π-acidic pyrazinyl rings could in principle engage in anion–π(pyrazinyl)<sup>5</sup> or S–π(pyrazinyl)<sup>6</sup> interaction for the supramolecular assembly.

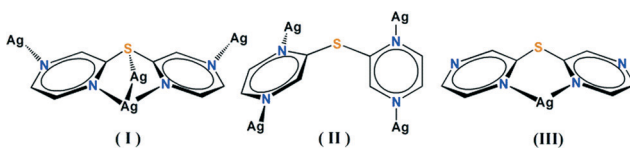
In this work, we report the synthesis and characterization of a series of Ag(i) CPs based on the new angular DpzS, namely,  $\{[Ag_3(DpzS)_2(ClO_4)_2](ClO_4)_2\}_{\infty}$  (1),  $[Ag_3(DpzS)_2(CF_3SO_3)_3]_{\infty}$  (2),  $\{[Ag_3(DpzS)_2(CF_3SO_3)(H_2O)_2](CF_3SO_3)_2 \cdot H_2O\}_{\infty}$  (3),  $[Ag_2(DpzS)(NO_3)_2(H_2O)]_{\infty}$  (4),  $[Ag(DpzS)(NO_2)]_{\infty}$  (5),  $[Ag_2(DpzS)(NO_2)_2]_{\infty}$  (6) and  $[Ag_2(DpzS)(C_2F_5CO_2)_2]_{\infty}$  (7). These CPs were characterized by single crystal X-ray diffraction, IR spectroscopy and elemental analyses. The role of the anions in determining the structure motifs has been discussed. In addition, the subtle tuning of the weak interactions, such as S–π(pyrazinyl) and anion–π(pyrazinyl), has also been investigated in these supramolecular architectures.

*Beijing Key Laboratory for Optical Materials and Photonic Devices, Department of Chemistry, Capital Normal University, Beijing 100048, PR China.*

E-mail: wancq@cnu.edu.cn; Fax: +86 010 68902320; Tel: +86 010 68903033 802

† Dedicated to Professor James Trotter on the occasion of his 80th birthday.

‡ Electronic supplementary information (ESI) available: The selected bond lengths and angles of the complexes 1–7 and ligand DpzS are listed in Table S1. CCDC 926723, 926718, 926719, 743076, 926720–926723. Crystallographic data for the structures reported in this paper have been deposited in the Cambridge Crystallographic Data Center as a supplementary publication. For ESI and crystallographic data in CIF or other electronic format see DOI: 10.1039/c3ce42404a



Scheme 1 Coordination modes of DpzS in 1–7.

## Experimental section

### Materials and physical measurements

All organic reagents were obtained through commercial source and used without further purification, and all of the metal salts were also obtained from commercial sources. Ligand DpzS was synthesized according to the reported procedure,<sup>4</sup> the details of which are shown in the ESI.‡ Elemental analyses (C, H, N) of all complexes were performed using an Elemental Vario EL analyzer. FT-IR spectra were recorded on a Bruker Equinox 55FT-IR spectrometer with dry KBr pellet in the range of 400–4000 cm<sup>-1</sup>. Powder X-ray diffraction (PXRD) patterns were recorded on a Bruker D8 Advance Powder X-ray diffractometer (Cu K $\alpha$ ,  $\lambda = 1.5418 \text{ \AA}$ ) operating at 40 kV and 40 mA, equipped with a graphite reflected beam monochromator and variable divergence slits. The peak positions of the simulated and experimental XRPD patterns are in good agreement with each other (Fig. 1).

### Syntheses of complexes 1–7

$\{[\text{Ag}_3(\text{DpzS})_2(\text{ClO}_4)_2](\text{ClO}_4)\}_{\infty}$  (1). A mixture of DpzS (18 mg, 0.1 mmol) and AgClO<sub>4</sub> (42 mg, 0.2 mmol) was dissolved in a mixed solvent of 2 ml of methanol and 3 ml of acetonitrile at room temperature. After 3 h, the colorless solution was filtered and slowly evaporated in air. Colorless crystals of 1 suitable for X-ray crystallographic analysis were deposited after one week. Yield: 40 mg (80% based on DpzS). Elemental anal. calcd (found) for C<sub>16</sub>H<sub>12</sub>Cl<sub>3</sub>N<sub>8</sub>O<sub>12</sub>S<sub>2</sub>Ag<sub>3</sub>: C, 19.15 (19.07); H, 1.20 (1.20); N, 11.17 (11.20). Selected IR data (KBr, pellet,  $\nu$  cm<sup>-1</sup>): 3432(m), 3219(m), 1630(m), 1506(w), 1456(w), 1397(vs), 1291(w), 1083(vs), 1009(m), 858(m), 834(m), 743(m), 626(vs), 547(m).

$[\text{Ag}_3(\text{DpzS})_2(\text{CF}_3\text{SO}_3)_3]_{\infty}$  (2). The synthesis procedure of 2 was the same as that for 1 except that AgClO<sub>4</sub> was replaced by

AgCF<sub>3</sub>SO<sub>3</sub> (52 mg, 0.2 mmol). Colorless crystals of 2 suitable for X-ray crystallographic analysis were obtained after one week. Yield: 34 mg (59% based on DpzS). Elemental anal. calcd (found) for C<sub>19</sub>H<sub>12</sub>F<sub>9</sub>N<sub>8</sub>O<sub>9</sub>S<sub>5</sub>Ag<sub>3</sub>: C, 19.80 (19.73); H, 1.04 (1.04); N, 9.73 (9.69). Selected IR data (KBr, pellet,  $\nu$  cm<sup>-1</sup>): 3119(m), 1632(m), 1511(w), 1461(m), 1401(vs), 1253(vs), 1160(s), 1030(s), 853(m), 757(m), 638(s), 572(m), 518(m).

$\{\text{Ag}_3(\text{DpzS})_2(\text{CF}_3\text{SO}_3)(\text{H}_2\text{O})_2\}[\text{CF}_3\text{SO}_3]_2\text{H}_2\text{O}\}_{\infty}$  (3). The synthesis procedure of 3 was the same as that for 2 except that 1 ml deionized water was added to the mixed solvent. Colorless crystals of 3 suitable for X-ray crystallographic analysis were deposited after one week by slow evaporation of the solvent in air. Yield: 31.8 mg (53% based on DpzS). Elemental anal. calcd (found) for C<sub>19</sub>H<sub>18</sub>Ag<sub>3</sub>F<sub>9</sub>N<sub>8</sub>O<sub>12</sub>S<sub>5</sub>: C, 18.92 (18.89); H, 1.49 (1.49); N, 9.29 (9.30). Selected IR data (KBr, pellet,  $\nu$  cm<sup>-1</sup>): 3440(m), 3110(m), 1630(m), 1506(m), 1462(vs), 1405(vs), 1250(m), 1163(s), 1034(m), 860(m), 756(m), 640(s), 570(m).

$[\text{Ag}_2(\text{DpzS})(\text{NO}_3)_2(\text{H}_2\text{O})]_{\infty}$  (4). The synthesis procedure of 4 was the same as that for 1 except that AgClO<sub>4</sub> (42 mg, 0.2 mmol) was replaced by AgNO<sub>3</sub> (17 mg, 0.1 mmol). Prism-like crystals of 4 were obtained through slow evaporation of the filtrate in air. Yield: 35 mg (64% based on DpzS). Elemental anal. calcd (found) for C<sub>8</sub>H<sub>8</sub>N<sub>6</sub>O<sub>7</sub>SAg<sub>2</sub>: C, 17.52 (17.47); H, 1.46 (1.46); N, 15.33 (15.30). Selected IR data (KBr, pellet,  $\nu$  cm<sup>-1</sup>): 3436(m), 2427(w), 1762(w), 1630(w), 1505(w), 1384(vs), 1008(m), 1119(s), 1051(m), 1009(m), 856(m), 835(m), 824(m), 743(m).

$[\text{Ag}(\text{DpzS})(\text{NO}_2)]_{\infty}$  (5). A mixture of DpzS (18 mg, 0.1 mmol) and AgNO<sub>2</sub> (15 mg, 0.1 mmol) was dissolved in a mixed solvent of 1 ml acetonitrile and 4 ml methanol with stirring at room temperature. Slow evaporation of the filtrate gave colorless crystals of 5. Yield: 4 mg (12% based on DpzS). Elemental anal. calcd (found) for C<sub>8</sub>H<sub>6</sub>N<sub>5</sub>O<sub>2</sub>SAg: C, 27.90 (27.77); H, 1.74 (1.75); N, 20.34 (20.39). Selected IR data (KBr, pellet,  $\nu$  cm<sup>-1</sup>): 3436(vs), 1632(m), 1507(m), 1454(m), 1385(s), 1270(s), 1121(m), 1050(m), 1010(m), 835(w), 743(w), 598(w).

$[\text{Ag}_2(\text{DpzS})(\text{NO}_2)]_{\infty}$  (6). A mixture of DpzS (18 mg, 0.1 mmol) and AgNO<sub>2</sub> (30 mg, 0.2 mmol) was dissolved in a mixed solvent of 1 ml acetonitrile and 5 ml methanol with stirring at room temperature. Slow evaporation of the filtrate gave colorless crystals of 6. Yield: 12 mg (24% based on DpzS). Elemental anal. calcd (found) for C<sub>8</sub>H<sub>6</sub>N<sub>6</sub>O<sub>4</sub>SAg<sub>2</sub>: C, 19.28 (19.29); H, 1.20 (1.21); N, 16.87 (16.90). Selected IR data (KBr, pellet,  $\nu$  cm<sup>-1</sup>): 3436(s), 1630(m), 1505(m), 1456(m), 1391(s), 1270(vs), 1120(s), 1053(m), 1010(s), 834(w), 743(w), 432(w).

$[\text{Ag}_2(\text{DpzS})(\text{C}_2\text{F}_5\text{CO}_2)]_{\infty}$  (7). A mixture of DpzS (18 mg, 0.1 mmol) and AgC<sub>2</sub>F<sub>5</sub>CO<sub>2</sub> (44 mg, 0.2 mmol) was dissolved in a mixed solvent of 4 ml acetonitrile and 1 ml methanol with stirring at room temperature for 30 minutes. After filtration, ether as the guest component was carefully layered over the resulting yellow solution to form an upper layer. Slow diffusion of ether molecules into the solution of the mixed solvent of acetonitrile and methanol over a period of 2 weeks yielded colorless crystals of 7. Yield: 45 mg (61% based on DpzS). Elemental anal. calcd (found) for C<sub>14</sub>H<sub>6</sub>N<sub>4</sub>O<sub>4</sub>SF<sub>10</sub>Ag<sub>2</sub>: C, 22.95 (22.88); H, 0.82 (0.81); N, 7.65 (7.69). Selected IR data (KBr, pellet,  $\nu$  cm<sup>-1</sup>): 3417(s), 2920(m), 2850(m), 1681(vs), 1506(w),

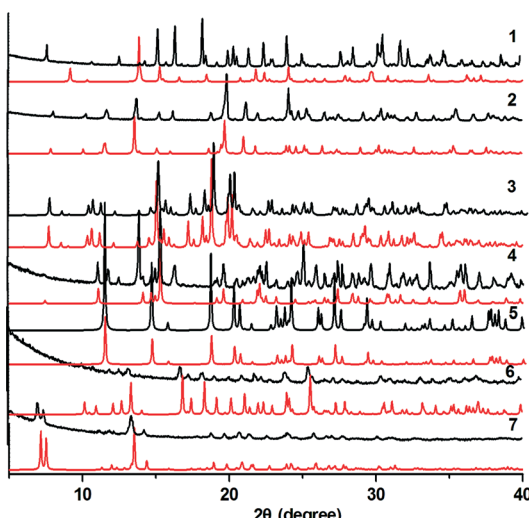


Fig. 1 Experimental (black) and simulated powder X-ray (red) diffraction patterns of complexes 1–7.

**Table 1** Crystallographic data of complexes 1–7

Complex	1	2	3	4	5	6	7
Empirical formula	$C_{16}H_{12}N_8O_{12}S_2Cl_3Ag_3$	$C_{19}H_{18}F_9N_8O_9S_5Ag_3$	$C_8H_8N_6O_7SAg_2$	$C_8H_6N_5O_2SAg$	$C_8H_6N_6O_4SAg_2$	$C_{14}H_6F_{10}N_4O_4SAg_2$	$C_8H_6N_6O_4SAg_2$
Formula weight	1002.42	1151.28	1205.31	548.00	344.11	497.99	732.03
Crystal system	Orthorhombic	Monoclinic	Triclinic	Monoclinic	Orthorhombic	Monoclinic	Monoclinic
Space group	<i>Imma</i>	<i>P1</i>	<i>Cc</i>	<i>Pmma</i>	<i>C2/c</i>	<i>C2/c</i>	<i>C2/c</i>
<i>a</i> /Å	19.181(4)	11.135(5)	8.9469(2)	8.5705(7)	18.4365(2)	18.7675(4)	
<i>b</i> /Å	9.4868(2)	12.380(6)	23.6973(6)	15.3195(1)	10.2983(9)	22.3080(4)	
<i>c</i> /Å	11.579(3)	15.7184(3)	7.3859(2)	8.4310(6)	15.905(3)	13.9336(5)	
$\alpha/^\circ$	12.642(3)	90	84.662(1)	90	90	90	90
$\beta/^\circ$	90	91.4760(1)	89.537(1)	108.400(2)	90	118.923(3)	128.1470(1)
$\gamma/^\circ$	90	90	67.261(1)	90	90	90	90
<i>V</i> /Å <sup>3</sup>	2808.0(1)	3317.49(1)	1848.3(2)	1485.88(6)	1106.95(2)	2643.1(5)	4587.6(2)
<i>Z</i>	4	4	2	4	4	8	8
<i>D</i> <sub>calc</sub> /g cm <sup>-3</sup>	2.371	2.305	2.162	2.450	2.065	2.503	2.120
$\mu$ (Mo-K $\alpha$ )/mm <sup>-1</sup>	2.581	2.180	1.967	2.825	2.006	3.146	1.908
<i>F</i> (000)	1936	2224	1168	1056	672	1904	2800
Reflections collected	7455	11014	12948	6427	4983	9335	20228
Independent reflections	1337(0.0457)	2870(0.0211)	9003(0.0376)	2929(0.0244)	1381(0.0189)	2310(0.0205)	5473(0.0372)
Observed reflections [ $I > 2\sigma(I)$ ]	1063	2562	5120	2651	1243	2133	2692
Parameters	128	264	532	218	89	199	316
Goodness-of-fit	1.081	1.063	1.018	1.030	1.051	1.036	1.042
$R_1$ [ $I > 2\sigma(I)$ ] <sup>a</sup>	0.337	0.0356	0.0588	0.0280	0.0231	0.0306	0.0574
wR <sub>2</sub> (all data) <sup>b</sup>	0.0848	0.0992	0.1577	0.0640	0.0591	0.0711	0.1868

<sup>a</sup>  $R_1 = \sum |F_o| - |F_c| / \sum |F_o|$ . <sup>b</sup> wR<sub>2</sub> =  $(\sum [w(F_o^2 - F_c^2)^2] / \sum [w(F_o^2)^2])^{1/2}$ .

1457(w), 1393(m), 1329(s), 1291(w), 1213(vs), 1163(vs), 1121(s), 1032(s), 1010(m), 835(m), 818(s), 732(s), 587(w), 540(w).

### X-Ray crystallographic study

Single-crystal X-ray diffraction data of DpzS and complexes 1–7 were collected on a Bruker APEX II CCD diffractometer, operating at 50 kV and 30 mA using Mo K $\alpha$  radiation ( $\lambda = 0.71073 \text{ \AA}$ ) at room temperature. Each selected crystal was mounted inside a Lindemann glass capillary, and each data reduction was performed using the SMART and SAINT software.<sup>7</sup> Empirical absorption correction was applied using the SADABS program.<sup>8</sup> All structures were solved by direct methods and refined by full-matrix least-squares on  $F^2$  using the SHELXTL program package.<sup>9</sup> The non-hydrogen atoms in each structure were refined with anisotropic displacement parameters, while the hydrogen atoms were placed in idealized positions and allowed to ride on the relevant carbon atoms. Except for the positions of the hydrogen atoms of O3W in 3 which cannot be located, all positions of the hydrogen atoms of the water molecules in 3 and 4 were obtained from different Fourier-difference maps and included in the final formula refinement. In 1, the Cl1-containing perchlorate has 1/4 fractional occupancy with O2 (1/2 occupancy) and O3 (1/4 occupancy) atoms exhibiting orientational disorder, while the O4 atom of the Cl2-containing perchlorate exhibits an orientational disorder with half fractional occupancy. In 2, the S3-containing triflate takes a half fractional occupancy, with S3, C10, F5, F6, O4 and O5 exhibiting orientational disorder. For complex 3, the S5, O8 and O9 atoms are disordered at two positions with equal ratios. In 5, the nitrite has half fractional occupancy with the nitrite N3 atom disordered at two sites with a ratio of 4:1. In complex 6, the nitrite N5 is disordered at two positions with a ratio of 4:1.<sup>8</sup> Crystallographic data with CCDC no. 926725 for DpzS, 926718 for complex 1, 926719 for 2, 743076 for 3, 926720 for 4, 926721 for 5, 926722 for 6 and 926723 for 7 (Table 1). Selected bond lengths and bond angles for DpzS and complexes 1–7 are listed in Table S1 (ESI).<sup>†</sup>

## Results and discussion

### Description of crystal structures

$\{[\text{Ag}_3(\text{DpzS})_2(\text{ClO}_4)_2](\text{ClO}_4)\}_{\infty}$  (1). As shown in Fig. 2a, there are three independent Ag(i) atoms (Ag1, Ag2 and Ag3) in the asymmetric unit of complex 1. The three Ag(i) atoms show two types of coordination geometries. Ag1 exhibits a square planar geometry, completed by four 4-pyrazinyl N atoms from four independent DpzS ligands. Ag2 and Ag3 show similar square pyramid geometry, but their coordination environments are different. Ag2 is coordinated by four 2-pyrazinyl N atoms from two different DpzS ligands. However, Ag3 is coordinated by two S atoms from two DpzS ligands chelating to the Ag2 (Ag-S 2.507(3)  $\text{\AA}$ ), and two O atoms from two different  $\text{ClO}_4^-$  anions (Cl2-containing).

<sup>†</sup>The structure of the DpzS ligand was also determined, and the crystal data and structure discussion were provided in the ESI.

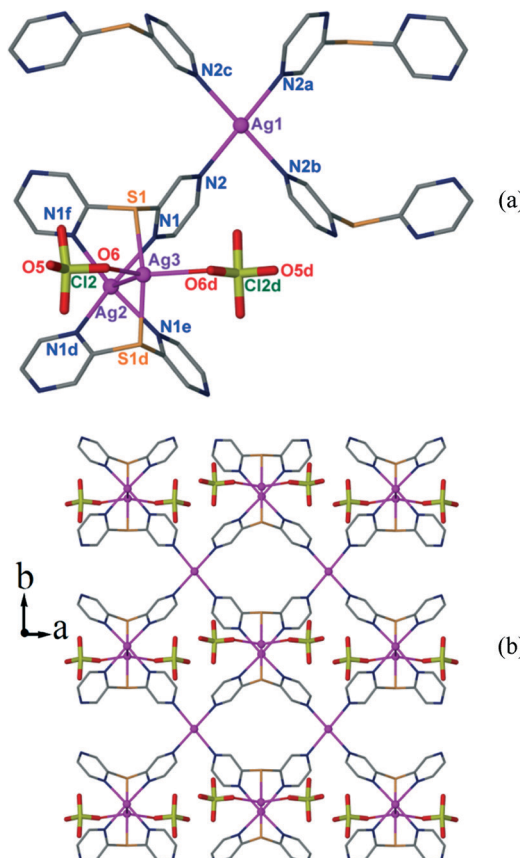
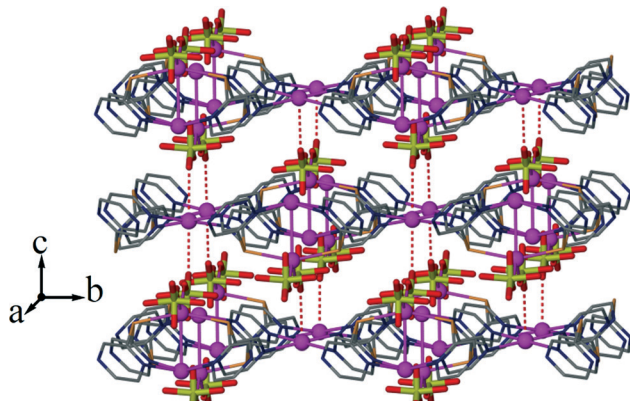


Fig. 2 (a) The coordination environments of silver(i) in 1. Symmetry codes: (a)  $-x + 3/2, -y + 3/2, -z + 3/2$ ; (b)  $-x + 3/2, y, -z + 3/2$ ; (c)  $x, -y + 3/2, z$ ; (d)  $-x + 1, -y + 1/2, z$ ; (e)  $x, -y + 1/2, z$ ; (f)  $-x + 1, y, z$ . (b) Two-dimensional cationic network of 1 viewed along the c axis.

Further, the square pyramid geometries of Ag2 and Ag3 were completed by the argentophilic interaction with an  $\text{Ag}\cdots\text{Ag}$  distance of 2.992(4) (Fig. 2a). Two DpzS (mode I in Scheme 1) chelate Ag2 and Ag3 to give a  $[\text{Ag}_2(\text{DpzS})_2(\text{ClO}_4)_2]$  unit, and the four free 4-pyrazinyl N atoms link four symmetry related Ag1 atoms to yield a 2-D layer with the Cl2-containing perchlorates arranged on both sides (Fig. 2b). Along the *c* direction, the formed layers are stacked to generate a 3-D supramolecular architecture, with the Cl1-containing perchlorate anions embedded in the interstices between the layers. Weak  $\text{Ag}1\cdots\text{O}5a(\text{ClO}_4^-)$  (2.786(4)  $\text{\AA}$ ) and  $\text{C}2-\text{H}\cdots\text{O}6b(\text{ClO}_4^-)$  hydrogen-bonding interactions are found to stabilize the full supramolecular structure ( $\text{D}\cdots\text{A}$  3.412(8)  $\text{\AA}$ ,  $\text{D}-\text{H}\cdots\text{A}$  163.13(3) $^\circ$ ). Symmetry codes: (a)  $x + 1/2, y + 1/2, z - 1/2$ ; (b)  $-x + 1, -y + 1, -z + 2$  (Fig. 3).

$[\text{Ag}_3(\text{DpzS})_2(\text{CF}_3\text{SO}_3)_3]_{\infty}$  (2). In the asymmetric unit of 2, two independent Ag(i) ions exhibit different coordination environments. Ag1 takes a  $\text{N}_2\text{O}_2$ -coordination environment with two 4-pyrazinyl N atoms from two different DpzS ligands and two symmetric triflate O1(S2-containing) with an  $\text{Ag}\cdots\text{O}$  distance of 2.673(3)  $\text{\AA}$ . However, Ag2 is coordinated by two 2-pyrazinyl N atoms and one 4-pyrazinyl N atom of three separate DpzS ligands, and one O5(S3-containing) at  $\text{Ag}\cdots\text{O} = 2.609(4) \text{\AA}$  to form a  $\text{N}_3\text{O}$ -coordination environment (Fig. 4a). Different from the coordination mode (I) of DpzS in 1, each



**Fig. 3** 3-D supramolecular architecture formed by Ag...O interactions (red-dashed lines) between the neighboring 2-D cationic layer structures in **1**. All C-H...O interactions, hydrogen atoms and Cl<sup>-</sup>-containing perchlorates are omitted for clarity.

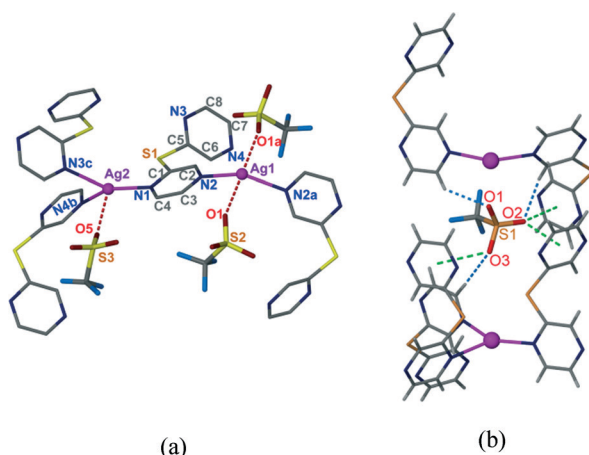


**Fig. 4** (a) Coordination geometries of Ag(I) centers in **2**. Symmetry codes: (a)  $-x + 1, y, -z + 1/2$ ; (b)  $x, -y, z + 1/2$ ; (c)  $-x + 1/2, -y + 1/2, -z + 1$ . (b) The O(triflate)... $\pi$  (green-dashed lines) and C–H...O (blue-dashed lines) interactions in **2** ( $C_2$ –H...O<sub>2d</sub>: D...A, 3.316(3) Å, D–H...A, 163.12(7) $^\circ$ ;  $C_3$ –H...O<sub>1</sub>: D...A, 3.161(3) Å, D–H...A, 137.25(4) $^\circ$ ;  $C_7$ –H...O<sub>3e</sub>: D...A, 3.347(2) Å, D–H...A, 172.30(1) $^\circ$ ). Symmetry codes: (d)  $-x + 1, y, -z + 1/2$ ; (e)  $x - 1/2, -y + 1/2, z - 1/2$ .

DpzS in **2** bridges four independent Ag(I) ions in a new  $\mu_4$ -bridging mode (II) (Scheme 1) through its four pyrazinyl N atoms to furnish a 3-D framework (Fig. 5a). The disordered S3-containing triflate anions are accommodated within the channel region, while the S2-containing triflate that links to the Ag1 atom exhibits C–H...O(triflate) and O(triflate)... $\pi$ (pyrazinyl) interactions with O...centroid(pyrazinyl) distances of 2.962(2), 3.174(3) and 3.499(3) Å (Fig. 4b).<sup>5,10</sup>

Topologically, if each DpzS and Ag2 is considered as a 4- and 3-connected node, respectively, the overall structure of **2** can be described as a 3-D (3,4)-connected net with a Schläfli symbol of {4·6·8}{4·6<sup>2</sup>·8<sup>3</sup>} (Fig. 5).<sup>11,12</sup>

$[\text{Ag}_3(\text{DpzS})_2(\text{CF}_3\text{SO}_3)(\text{H}_2\text{O})_2](\text{CF}_3\text{SO}_3)_2 \cdot \text{H}_2\text{O}$  (3). In the asymmetric unit of **3**, there are three independent Ag(I) atoms. All of the Ag(I) atoms are four-coordinated in tetrahedral geometries, but the coordination environments of Ag2 and Ag3

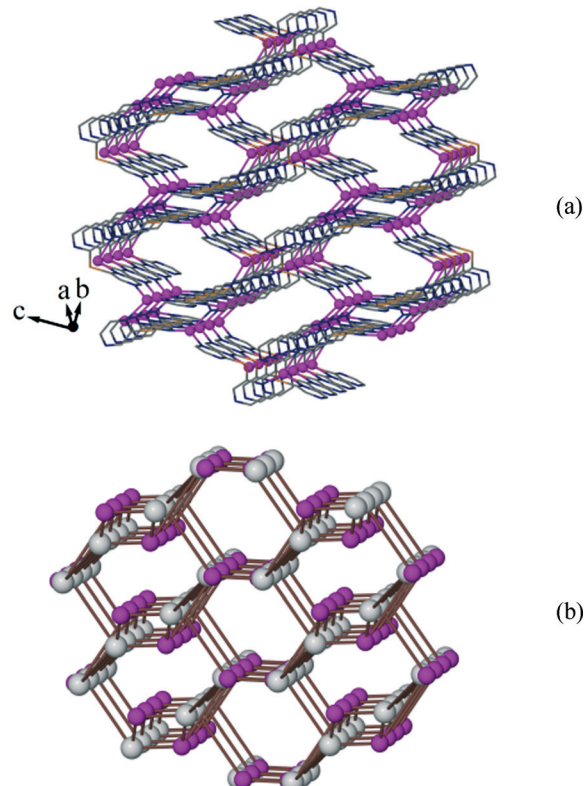


**Fig. 5** (a) 3-D framework of **2**. The silver(I) ions are shown as purple balls, and all hydrogen atoms and triflate are omitted for clarity. (b) The rationalized topological network in **2**. The purple balls represent Ag2 nodes, while the white balls represent DpzS.

are different from that of Ag1. As shown in Fig. 6, Ag1 is coordinated by two 2-pyrazinyl N atoms and two independent aqua ligands to achieve a  $N_2O_2$ -coordination environment. However, both Ag2 and Ag3 are surrounded by one triflate O atom, two 4-pyrazinyl N atoms and one 2-pyrazinyl N atom from two different DpzS ligands to give  $N_3O$ -coordination geometries.

Similar to that in **2**, each DpzS in **3** also links four Ag(I) ions in a  $\mu_4$ -bridging mode (II) with its four pyrazinyl N atoms, leading to a porous 3-D framework with a channel structure (Fig. 7a). The S3-, S4- and S5-containing triflate anions are accommodated within the channels. In addition, the S3-containing triflate exhibits C–H...O(triflate) and O(triflate)... $\pi$ (pyrazinyl) interactions with O...centroid(pyrazinyl) distances of 3.398(6) and 3.421(5) Å. The S4-containing triflate accommodates within the channels via C–H...O(triflate), O(aqua)–H...F(triflate), Ag...O(triflate) and O(triflate)... $\pi$ (pyrazinyl) interactions with a O...centroid(pyrazinyl) distance of 3.034(7) Å, while the S5-containing triflate attaches to the electron-deficient framework through O(aqua)–H...O(triflate), O(aqua)–H...F(triflate) and O(triflate)... $\pi$ (pyrazinyl) interactions with a O...centroid(pyrazinyl) distance of 3.197(2) Å (Fig. 6b).

From a view of topology, if each DpzS is regarded as a 4-connected node, and Ag2 and Ag3 are both considered as 3-connected nodes, the overall structure of **3** can be described as a 3-D (3,4)-connected net with a Schläfli symbol of {4·6·8}{4·6<sup>2</sup>·8<sup>3</sup>} (Fig. 7b).<sup>11</sup>

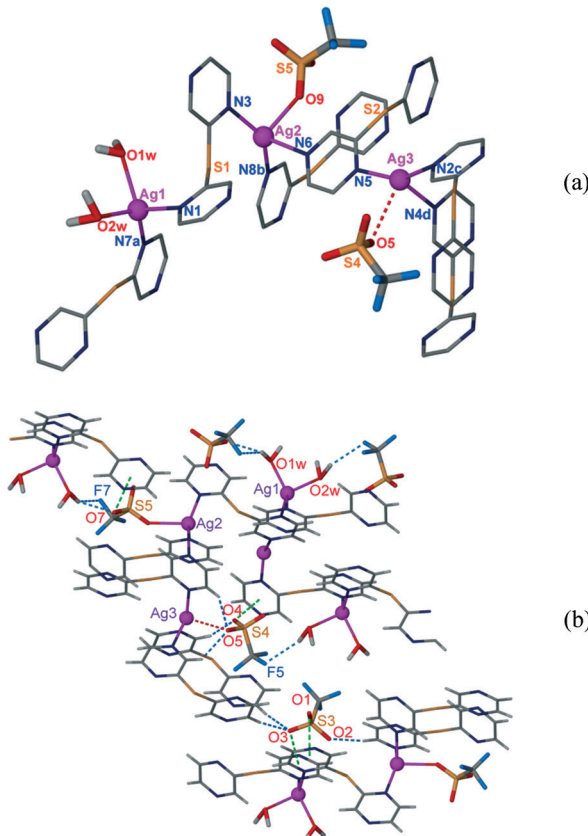


**Fig. 6** (a) Coordination geometries of Ag(I) centers in 3. Symmetry codes: (a)  $x + 1, y - 1, z$ ; (b)  $-x + 1, -y + 1, -z + 2$ ; (c)  $-x + 1, -y + 1, -z + 1$ ; (d)  $x - 1, y, z$ . (b) The O(triflate)···π (green-dashed lines), C-H···O (C2-H···O4a: D···A, 3.087(1) Å, D-H···A, 146.0(2)°; C6-H···O5b: D···A, 3.247(1) Å, D-H···A, 134.7(6)°; C12-H···O5: D···A, 3.183(1) Å, D-H···A, 134.4(3)°), O-H···F (O1W-H1WB···F7c: D···A, 3.340(1) Å, D-H···A, 149.5(4)°), O-H···O (O1W-H1WB···O7d: D···A, 2.890(1) Å, D-H···A, 118.2(5)°) (blue-dashed lines) and Ag···O (red-dashed lines) interactions in 3. Symmetry codes: (a)  $-x + 1, -y + 1, -z + 1$ ; (b)  $x + 1, y, z$ ; (c)  $-x + 2, -y + 1, -z + 2$ ; (d)  $-x + 2, -y + 2, -z + 2$ .

[Ag<sub>2</sub>(DpzS)(NO<sub>3</sub>)<sub>2</sub>(H<sub>2</sub>O)]<sub>∞</sub> (4). There exist two independent silver(I) atoms (Ag1 and Ag2) in the asymmetric unit cell of 4. Both Ag1 and Ag2 are four-coordinated in tetrahedral geometries, but they show different coordination environments. As shown in Fig. 8, Ag1 atom is surrounded by three 4-pyrazinyl N atoms from three different DpzS ligands and one independent aqua ligand. However, Ag2 is coordinated by one 4-pyrazinyl N atom and three O atoms from two terminal nitrate groups ( $\eta^1$ -O and  $\kappa^2$ O,O' nitrate). Ag1 and Ag2 atoms are linked by DpzS in  $\mu_4$ -bridging mode II (Scheme 1) to yield a 2-D layer (Fig. 9a). If Ag1 and DpzS are both regarded as 3-connected nodes, the overall structure of 4 is a 2-D 3-connected uninode topological {6<sup>3</sup>} hcb network (Fig. 9b).<sup>13</sup>

Interestingly, the  $\eta^1$ -O and  $\kappa^2$ O,O' nitrate groups arranged on both sides of the 2-D layer approach toward the opposite layers and contact with the pyrazinyl rings via O(NO<sub>3</sub>)<sup>-</sup>···π(pyrazinyl) [O(O1/O5/O6)···centroid(pyrazinyl)] distances range from 2.991(2) to 3.303(6) Å and H-bonding interactions [O1W-H1WA···O4a: D···A, 2.805(7) Å, D-H···A, 142.12(3)°; O1W-H1WB···O2b: D···A, 2.918(6) Å, D-H···A, 132.89(2)°].

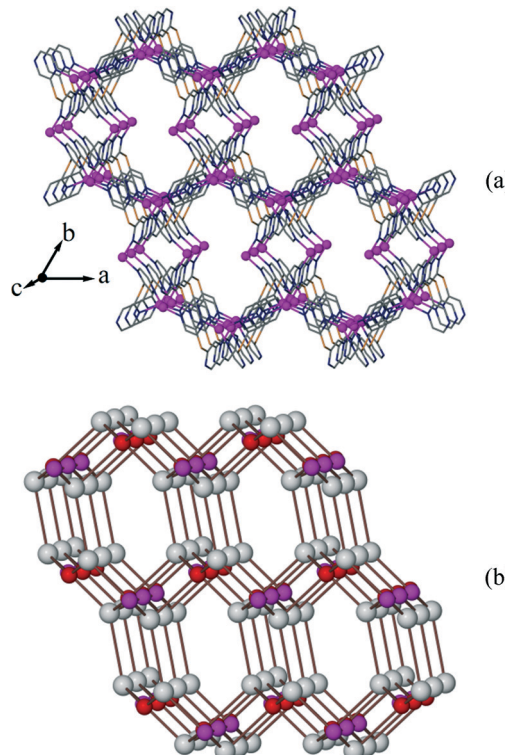


**Fig. 7** (a) 3-D framework of 3. All hydrogen atoms and triflate anions are omitted for clarity. (b) The rationalized topological network in 3. The purple balls indicate Ag2, the red balls indicate Ag3, and the white balls represent DpzS.

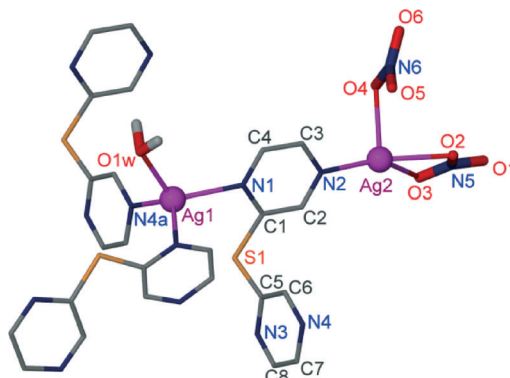


**Fig. 8** Coordination environments of Ag(I) atoms in 4. Symmetry codes: (a)  $x, y, z + 1$ ; (b)  $x + 1/2, -y + 1/2, z + 1/2$ .

O1W-H1WB···O1b: D···A, 3.108(7) Å, D-H···A, 168.44(4)°], as shown in Fig. 10a. Therefore, the layers are stacked along the *b* axis and interconnected through aforementioned non-covalent interactions to furnish a 3-D supramolecular architecture, as shown in Fig. 10b.

[Ag(DpzS)(NO<sub>2</sub>)]<sub>∞</sub> (5). In complex 5, Ag1 is chelated by two 2-pyrazinyl N atoms of the DpzS ligand and is further bonded to one N3 atom of a nitrite (Fig. 11a). Structure analysis reveals that the nitrite also exhibits Ag1···O1b interactions with Ag···O of 2.647(5) Å (b:  $x - 1/2, y, -z + 3/2$ ), thus the Ag1 can be viewed as a N<sub>3</sub>O<sub>2</sub>-coordination geometry surrounded by two  $\mu_2$ -N,O,O'-bridging nitrite groups and one

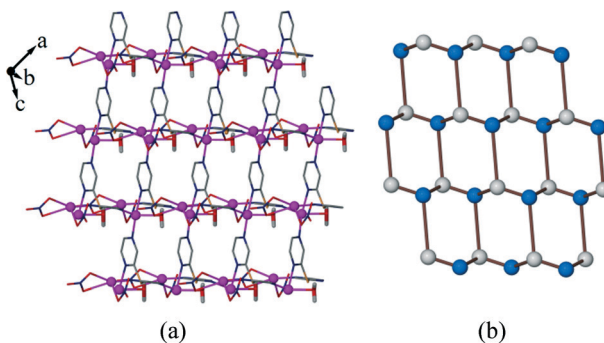


**Fig. 9** (a) 2-D layer-like structure in 4. The Ag<sup>(I)</sup> ions are shown as purple balls, and all hydrogen atoms on the pyrazinyl ring are omitted for clarity. (b) The rationalized topological structure of 4. The blue balls represent Ag1 nodes, while the white balls indicate the DpzS nodes.

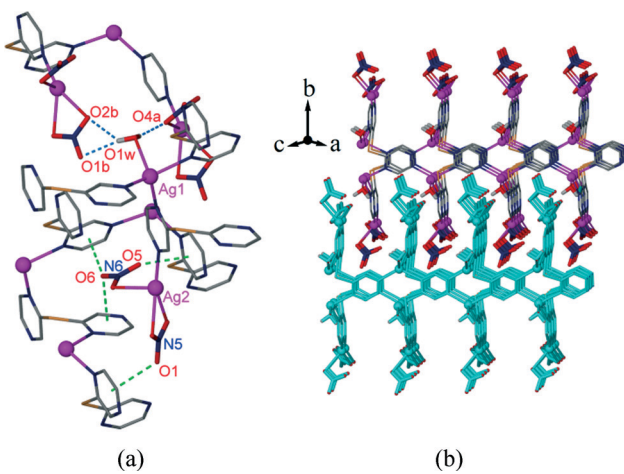


**Fig. 10** (a) O<sup>-</sup>···π (green-dashed lines) and H-bonding (blue-dashed lines) interactions in 4. Symmetry codes: (a)  $x + 1, -y + 1, z + 1/2$ ; (b)  $x + 1, -y + 1, z + 3/2$ . (b) 3-D supramolecular architecture of 4. All hydrogen atoms on the pyrazinyl ring are omitted, and adjacent layers are shown as different colors for clarity.

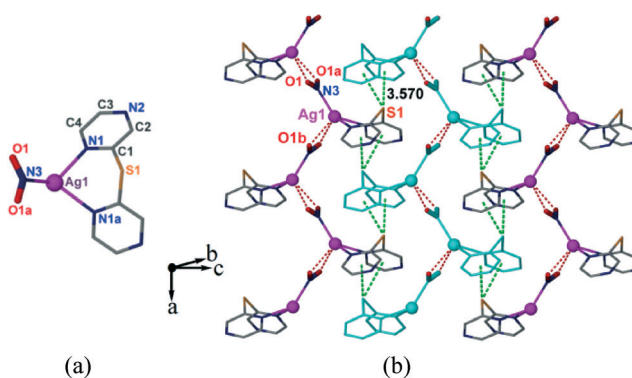


**Fig. 11** (a) Coordination geometry of Ag<sup>(I)</sup> center in 5. Symmetry code: (a)  $x, -y + 1/2, z$ . (b) The layer-like coordination motif in 5. The red-dashed lines represent Ag···O bonding (Ag···O = 2.647(5) Å), while the green-dashed lines indicate π···S···π interactions.

$\kappa^2\text{N,N}$ -chelating DpzS (mode III, Scheme 1). The  $\mu_2\text{-N,O,O}'$ -bridging nitrite groups link the Ag<sup>(I)</sup> centers to form an infinite zigzag chain along the  $a$  axis. Interestingly, the S atoms on the chain contact with the pyrazinyl rings of

adjacent chains through attractive  $\pi\cdots\text{S}\cdots\pi$  ( $\text{S}\cdots\text{centroid} = 3.570(3)$  Å) interactions to form a layer-like motif in the  $ac$  plane (Fig. 11b). Such a  $\text{S}\cdots\pi$  interaction belongs to lone-pair aromatic interaction, and the  $\pi\cdots\text{S}\cdots\pi$  contact mode (centroid···S···centroid angle =  $85.85(6)^\circ$ ) is similar to that in crystalline sulfanyl-triazine derivatives.<sup>14</sup>

The 2-D layer structures are stacked along the  $b$  axis and interconnected *via* intermolecular C-H···N and C-H···O(nitrite) hydrogen bonding (C4-H···N2a: D···A, 3.398(2) Å, D-H···A, 129.87(3)°; C3-H···O1b: D···A, 3.458(3) Å, D-H···A, 146.93(1)°. Symmetry codes: (a)  $-x + 1/2, -y + 1, z + 1/2$ ; (b)  $-x + 1, -y + 1, -z + 1$ ) interactions, leading to a 3-D supramolecular architecture, as shown in Fig. 12.

[Ag<sub>2</sub>(DpzS)(NO<sub>2</sub>)<sub>2</sub>]<sub>∞</sub> (6). With respect to that of 5, a markedly different complex 6 was achieved through the variation of the reaction ratio of DpzS and AgNO<sub>2</sub>. As shown in Fig. 13, there are two independent Ag<sup>(I)</sup> atoms (Ag1 and Ag2) in the asymmetric unit of 6. Ag1 is coordinated by two

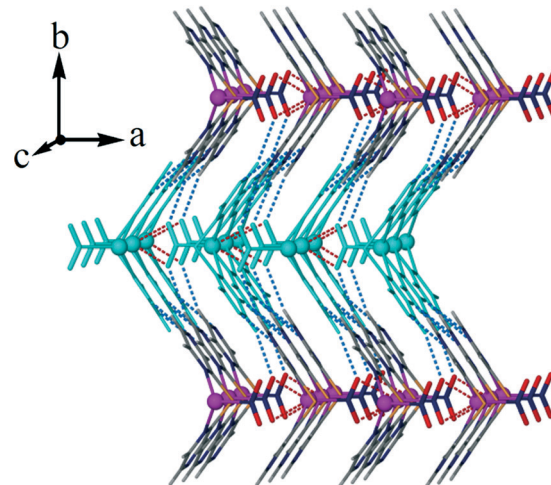


**Fig. 12** 3-D supramolecular architecture of 5 stacked by the 2-D layers. Red-dashed lines indicate Ag···O interactions, while the blue-dashed lines represent C-H···N and C-H···O(nitrite) interactions.

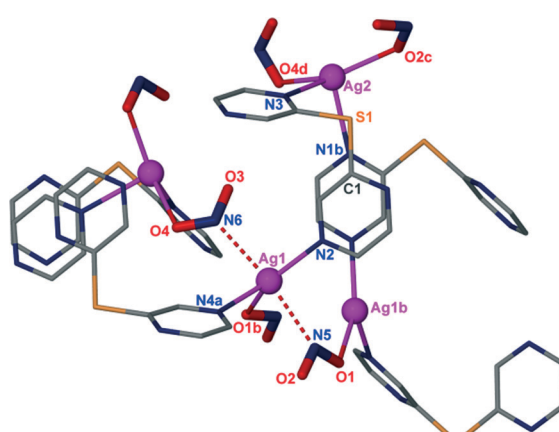


**Fig. 13** Coordination environments of Ag<sup>(I)</sup> in 6. Ag1···N6, 2.652(5) Å; Ag1···N5, 2.635(4) Å. Symmetry codes: (a)  $-x + 3/2, -y + 3/2, -z + 1$ ; (b)  $-x + 1, y, -z + 1/2$ ; (c)  $-x + 1, y - 1, -z + 1/2$ ; (d)  $-x + 3/2, y - 1/2, -z + 1/2$ .

4-pyrazinyl N atoms from two different DpzS ligands, one nitrite O atom, and two nitrite N atoms, leading to a distorted pyramidal  $\text{N}_4\text{O}$ -coordination geometry. Ag2 takes a distorted  $\text{N}_2\text{O}_2$ -tetrahedral coordination geometry with two 2-pyrazinyl N atoms from two different DpzS ligands and two nitrite O atoms around.

Notably, each DpzS ligand in 6 bridges four Ag(i) ions in the  $\mu_4$ -ligation mode II, which is completely different from that in 5 (mode III in Scheme 1). Interestingly, each N5-containing nitrite links two symmetry-related Ag1 and one Ag2 in a  $\mu_3\text{-N}, \text{O}, \text{O}'$ -bridging mode and combines with the  $\mu_4$ -bridging DpzS to fabricate a 2-D layer structure (Fig. 14a). However, the N6-containing nitrite anions are deposited on both sides of the formed layer. If DpzS and Ag1 are both regarded as a 4-connected node, while Ag2 and the  $\mu_3$ -bridging nitrite are both considered as 3-connected nodes, the overall structure of 6 can be described as a 2-D (3,4)-connected network with a Schläfli symbol of  $\{4\cdot6^2\}\{4^2\cdot6^2\cdot8^2\}$  (Fig. 14b).

As shown in Fig. 15, the N6-containing nitrite groups deposit on both sides of each layer and link adjacent layers through  $\text{Ag}1\cdots\text{N}6$  interactions ( $\text{Ag}\cdots\text{N} = 2.652(5)$  Å), resulting in a 3-D supramolecular architecture of 6.

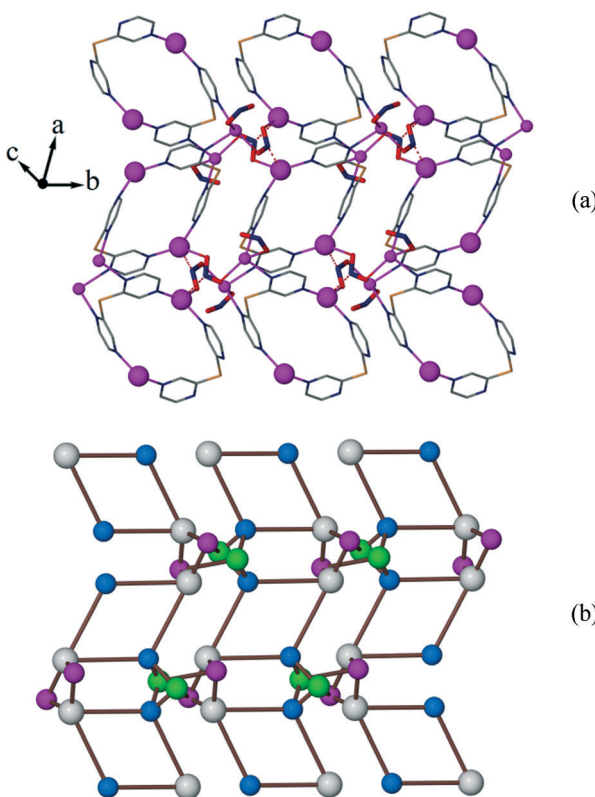


**Fig. 14** (a) 2-D layer structure of 6. The Ag1 atoms are shown as large purple balls, the Ag2 atoms are shown as small purple ones, and red-dashed lines indicate  $\text{Ag}\cdots\text{N}$ (N5-containing nitrites) interactions. (b) 2-D (3,4)-connected network with a Schläfli symbol of  $\{4\cdot6^2\}\{4^2\cdot6^2\cdot8^2\}$ . The blue balls represent Ag1 nodes, the purple balls indicate Ag2 nodes, the white balls indicate the DpzS, and the green nodes represent the  $\mu_3\text{-N}, \text{O}, \text{O}'$ -bridging nitrite.

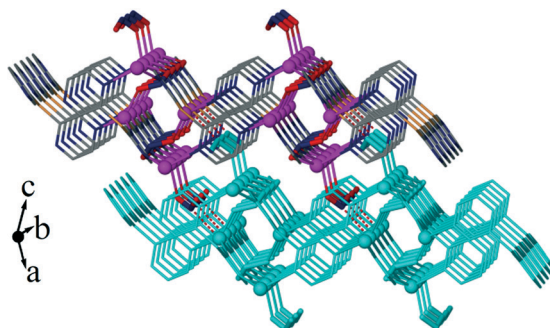


**Fig. 15** 3-D supramolecular architecture of 6 stacked by the 2-D layers. Red-dashed lines represent  $\text{Ag}1\cdots\text{N}6$  interactions.

**[ $\text{Ag}_2(\text{DpzS})(\text{C}_2\text{F}_5\text{CO}_2)_2$ ]<sub>∞</sub>** (7). In the asymmetry unit of 7, there exist two independent Ag(i) atoms (Ag1 and Ag2). Ag1 takes a distorted  $\text{N}_2\text{O}_2$ -coordination geometry, completed by two 2-pyrazinyl N atoms from two DpzS ligands and two O atoms from two separated pentafluoropropionates. Two pentafluoropropionates taking a *syn*- $\eta^1\cdot\eta^1\cdot\mu_2$ -bridging mode bridge Ag1 and its symmetry-related species to form a dinuclear Ag(i) cluster with an  $\text{Ag}1\cdots\text{Ag}1$ a distance of 3.313(4) Å. Ag2 exhibits a planar  $\text{N}_2\text{O}$ -coordination geometry with two 4-pyrazinyl N atoms from two DpzS ligands and one pentafluoropropionate O around (Fig. 16). Each DpzS ligand bridges four Ag(i) atoms in  $\mu_4$ -bridging mode II through its four pyrazinyl N atoms to yield a 3-D framework. The pentafluoropropionate anions are accommodated within the lattice cavities of the 3-D framework.

Topologically, treating each DpzS and Ag2 cluster as a 4-connected node, the structure of 7 can be described as a 4-connected mog net with a Schläfli symbol of  $\{4\cdot6^4\cdot8\}_2\{4^2\cdot6^2\cdot8^2\}$  (Fig. 17).<sup>15</sup>

#### Anion effect on the structures of 1–7

The counteranions  $\text{ClO}_4^-$  (in 1),  $\text{CF}_3\text{SO}_3^-$  (in 2 and 3),  $\text{NO}_3^-$  (in 4),  $\text{NO}_2^-$  (in 5 and 6) and  $\text{C}_2\text{F}_5\text{CO}_2^-$  (in 7) exhibit different

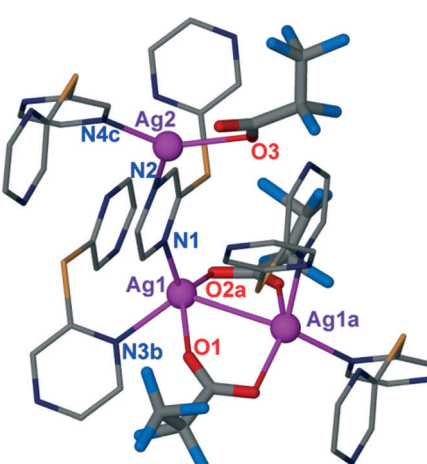


**Fig. 16** Coordination geometries of Ag(i) centers in 7. Symmetry codes: (a)  $-x + 1, y, -z + 3/2$ ; (b)  $-x + 1, -y + 1, -z + 1$ ; (c)  $x + 1/2, -y + 1/2, z + 1/2$ .

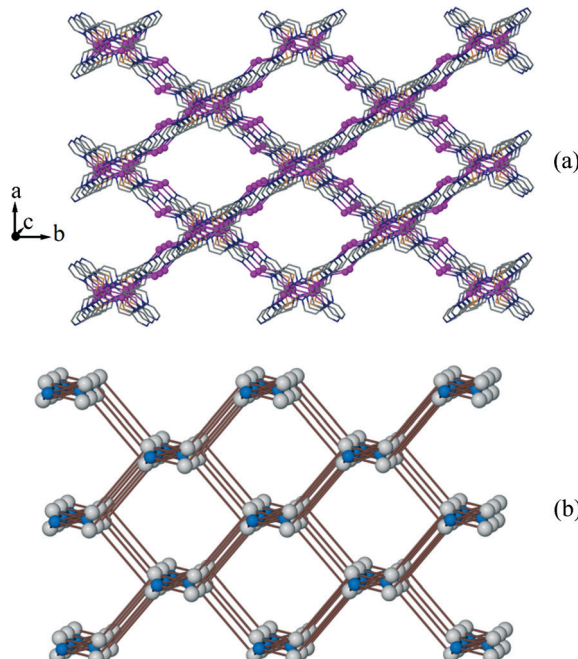


**Fig. 17** (a) 3-D framework of 7. All hydrogen atoms and triflates are omitted for clarity. (b) View of the 4-connected mog net with a Schläfli symbol of  $\{4.6^4.8\}_2\{4^2.6^2.8^2\}$ . The blue balls represent  $\text{Ag}_2$  cluster nodes, while the white balls indicate DpzS.

coordination abilities, electron densities, steric bulk, and molecular geometries, which have been rationally utilized to regulate the desired supramolecular architecture of various metal complexes.<sup>16</sup> In comparison, anions  $\text{ClO}_4^-$  and  $\text{CF}_3\text{SO}_3^-$  show relatively weak coordination ability with respect to the other anions.<sup>17</sup> Thus, in complexes 1–3, they weakly bond to  $\text{Ag}(\text{i})$  and/or are freely depositing among the interstices of their supramolecular architectures. On the contrary,  $\text{NO}_3^-$  in 4,  $\text{NO}_2^-$  in 5 and 6, and  $\text{C}_2\text{F}_5\text{CO}_2^-$  in 7 are involved in O–Ag bonding interactions. Therefore, it is understandable that the aqua ligands readily bond to the metal centre in 3, leading to the  $\text{N}_2(\text{H}_2\text{O})_2$ -geometry. In 3, the aqua ligands not only function as co-ligands but are also involved in H-bonding interactions to construct the supramolecular structure of 3. With respect to that of  $\text{NO}_3^-$ ,  $\text{NO}_2^-$  has a relatively small van der Waals volume and different geometry which has been rationally utilized as a versatile bridging co-ligand in a wide range of metal complexes.<sup>18</sup> In 4,  $\text{NO}_3^-$  acts as a  $\eta^1$ -O and  $\kappa^2$ O,O' terminal co-ligand in the distorted tetrahedral  $\text{N}_3\text{O}$ -coordination geometry, while  $\text{NO}_2^-$  in 5 functions in a  $\mu_2$ -N,O,O'-bridging mode to form the  $\text{N}_3\text{O}_2$ -coordination geometry. Nevertheless, the two  $\text{NO}_2^-$  groups in 6 exhibit  $\mu_2$ -N,O and  $\mu_3$ -N,O,O'-bridging modes (Fig. 13) to form  $\text{N}_4\text{O}$ - and  $\text{N}_2\text{O}_2$ -coordination geometries, respectively. It is clear that the flexible bridging modes of nitrites in 5 and 6 are responsible for the markedly different 3-D frameworks with respect to that of the nitrate in 4. As far as 5 and 6 are concerned, their different final structures can be ascribed to the different bridging nitrites and the distinct metal-to-ligand ratio of the starting materials. In contrast to the relatively weak coordination ability of the aforementioned

inorganic anions, such as  $\text{ClO}_4^-$ ,  $\text{CF}_3\text{SO}_3^-$ ,  $\text{NO}_3^-$  and  $\text{NO}_2^-$ , the carboxylate ligand has a relatively large steric bulk and strong coordination ability to the metal ions.<sup>13–15</sup> In 7, the two  $\text{C}_2\text{F}_5\text{CO}_2^-$  groups show  $\eta_1$ -O and *syn,syn*- $\eta^1:\eta^1:\mu_2$  bridging modes, respectively,<sup>19</sup> leading to a markedly different 3-D framework from those of 1–6.

### Anion– $\pi$ (pyrazinyl) interaction

The anion– $\pi$  contact is analogous to the lone-pair aromatic interaction that is of current interest because of its important role in supramolecular assembly.<sup>5,6</sup> In this work, the O(triflate)– $\pi$ (pyrazinyl) interaction is a common domain noncovalent interaction that engages in the formation of the supramolecular architectures of 2 and 3. As shown in Fig. 4 and 6, the O(triflate)– $\pi$ (pyrazinyl) distances range from 2.962(2) to 3.499(3) Å, which are around the sum of the O radius (1.40 Å)<sup>20</sup> and half the thickness of phenyl (1.84 Å)<sup>21</sup> and comparable to the O(triflate)– $\pi$ (pyrazinyl) distance of 3.380(5) Å in  $[\text{Ag}(\text{L})(\text{CF}_3\text{SO}_3)]_\infty$  ( $\text{L}$  = sulfonyldipyrazine).<sup>10</sup> In 4 (Fig. 10), the O( $\text{NO}_3^-$ )– $\pi$ (pyrazinyl) distances vary from 2.991(2) to 3.303(3) Å, which are comparable to the mean O( $\text{NO}_3^-$ )– $\pi$ (pyridine) distance of 3.302 Å as surveyed by Reedijk *et al.* through a CSD search.<sup>5a</sup>

### IR spectra of complexes 1–7

The IR spectra of 1–7 were recorded in the region of 400–4000 cm<sup>–1</sup> (Fig. S1).<sup>‡</sup> From the IR spectra of Fig. S1,<sup>‡</sup> it can be seen that the free ligand DpzS shows similar vibration peaks to those observed in its corresponding complexes 1–7. For example, the C=N vibrations of the free DpzS ligand are observed at 1505, 1457 and 1392 cm<sup>–1</sup>,<sup>3a</sup> and similar ones of its corresponding complexes 1–7 are around 1507, 1461 and 1397 cm<sup>–1</sup>, respectively. Moreover, there are two weak double bands around 841–861 cm<sup>–1</sup> and 730–756 cm<sup>–1</sup> in both complexes 1–7 and the free DpzS ligand, corresponding to the  $\delta(\text{C}-\text{S}-\text{C})$  bending and  $\nu(\text{C}-\text{S})$  stretching frequency, respectively.<sup>2d</sup>

### Conclusion

A series of silver(i) CPs constructed by a new multidentate di-2-pyrazinylsulfide (DpzS) ligand have been reasonably designed and synthesized. The DpzS ligand exhibits diverse coordination modes with various silver(i) salts, yielding fascinating 2-D and 3-D topological frameworks. Systematic investigations of their structural diversities indicate that the counteranions, as well as the size and geometry, play key roles in the formation of the final structural motifs of 1–7. In addition, the anion– $\pi$  contact, such as the anion– $\pi$ (pyrazinyl) interaction, also plays an important role in the supramolecular assembly of 1–7. Further studies on the new CPs based on a related angular multidentate ligand are under way.

### Acknowledgements

We acknowledge financial support from the Natural Science Foundation of Beijing Municipality (grant no. 2122011), the

National Natural Science Foundation of China (grant no. 21371123) and the Beijing Municipal Science & Technology Commission (Z131103002813097).

## Notes and references

- 1 (a) G. Tresoldi, E. Rotondo, P. Piraino, M. Lanfranchi and A. Tiripicchio, *Inorg. Chim. Acta*, 1992, **194**, 233–241; (b) G. Bruno, F. Nicolo, S. L. Schiavo, M. S. Sinicropi and G. Tresoldi, *J. Chem. Soc., Dalton Trans.*, 1995, 17–24; (c) G. Tresoldi, S. L. Schiavo, P. Piraino and P. Zanello, *J. Chem. Soc., Dalton Trans.*, 1996, 885–892; (d) G. Bruno, F. Nicolo, G. Tresoldi and S. Lanza, *Acta Crystallogr., Sect. C: Cryst. Struct. Commun.*, 2002, **58**, m56–m58; (e) L. Baradello, S. L. Schiavo, F. Nicolo, S. Lanza, G. Alibrandi and G. Tresoldi, *Eur. J. Inorg. Chem.*, 2004, 3358–3369.
- 2 (a) O.-S. Jung, S. H. Park, D. C. Kim and K. M. Kim, *Inorg. Chem.*, 1998, **37**, 610–611; (b) O.-S. Jung, Y. J. Kim, Y.-A. Lee, H. K. Chae, H. G. Jang and J. Hong, *Inorg. Chem.*, 2001, **40**, 2105–2110; (c) O.-S. Jung, Y. J. Kim, Y.-A. Lee, K.-M. Park and S. S. Lee, *Inorg. Chem.*, 2003, **42**, 844–850; (d) C.-Q. Wan, Z.-J. Wang, G. Wang, H. Liu, Y.-H. Deng and Q.-H. Jin, *Cryst. Growth Des.*, 2012, **12**, 376–386.
- 3 (a) R. Scopelliti, G. Bruno, C. Donato and G. Tresoldi, *Inorg. Chim. Acta*, 2001, **313**, 43–55; (b) G. Tresoldi, S. L. Schiavo, S. Lanza and P. Cardiano, *Eur. J. Inorg. Chem.*, 2002, 181–191.
- 4 (a) C.-Q. Wan, L. Zhao and T. C. W. Mak, *Inorg. Chem.*, 2010, **49**, 97–107; (b) X.-C. Jia, C. Chen, X. Li, B. Zhang and Y.-Y. Yu, *Z. Kristallogr. - New Cryst. Struct.*, 2013, **228**(3), 325–326.
- 5 (a) T. J. Mooibroek, C. A. Black, P. Gamez and J. Reedijk, *Cryst. Growth Des.*, 2008, **8**, 1082–1093; (b) P. Ballester, *Acc. Chem. Res.*, 2013, **46**, 874–884; (c) H. T. Chifotides and K. R. Dunbar, *Acc. Chem. Res.*, 2013, **46**, 894–906; (d) B. L. Schottel, H. T. Chifotides, M. Shatruk, A. Chouai, L. M. Pérez, J. Bacsa and K. R. Dunbar, *J. Am. Chem. Soc.*, 2006, **128**, 5895–5912; (e) D.-X. Wang, Q.-Y. Zheng, Q.-Q. Wang and M.-X. Wang, *Angew. Chem., Int. Ed.*, 2008, **47**, 7485–7488; (f) B. Han, J. Lu and J. K. Kochi, *Cryst. Growth Des.*, 2008, **8**, 1327–1334; (g) D.-X. Wang, Q.-Q. Wang, Y. Han, Y. Wang, Z.-T. Huang and M.-X. Wang, *Chem.-Eur. J.*, 2010, **16**, 13053–13057; (h) D.-X. Wang and M.-X. Wang, *J. Am. Chem. Soc.*, 2013, **135**, 892–897.
- 6 (a) L. Addadi and M. Lahav, *Pure Appl. Chem.*, 1979, **51**, 1269–1284; (b) I. Alkorta, I. Rozas and J. Elguero, *J. Org. Chem.*, 1997, **62**, 4687–4691; (c) C. Garau, A. Frontera, D. Quinonero, P. Ballester, A. Costa and P. M. Deya, *ChemPhysChem*, 2003, **4**, 1344–1348; (d) M. Egli and S. Sarkhel, *Acc. Chem. Res.*, 2007, **40**, 197–205; (e) T. J. Mooibroek, P. Gamez and J. Reedijk, *CrystEngComm*, 2008, **10**, 1501–1515.
- 7 SMART 5.0 and SAINT 4.0 for Windows NT, Area Detector Control and Integration Software, Bruker Analytical X-Ray Systems Inc., Madison, WI, 1998.
- 8 G. M. Sheldrick, SADABS: Program for Empirical Absorption Correction of Area Detector Data, University of Gottingen, Gottingen, Germany, 1996.
- 9 G. M. Sheldrick, *SHELXTL 5.1 for Windows NT: Structure Determination Software Programs*, Bruker Analytical X-ray Systems, Inc., Madison, WI, 1997.
- 10 C.-Q. Wan and T. C. W. Mak, *New J. Chem.*, 2011, **35**, 319–327.
- 11 (a) P. Feng, X.-H. Bu and N.-F. Zheng, *Acc. Chem. Res.*, 2005, **38**, 293–303; (b) L.-M. Fan, X.-T. Zhang, Z. Sun, W. Zhang, Y.-S. Ding, W. L. Fan, L.-M. Sun, X. Zhao and H. Lei, *Cryst. Growth Des.*, 2013, **13**, 2462–2475; (c) H. Reinsch, M. Kruger, J. Marrot and N. Stock, *Inorg. Chem.*, 2013, **52**, 1854–1859.
- 12 V. A. Blatov, Multipurpose crystallochemical analysis with the program package TOPOS, *IUCr CompComm Newsletter*, 2006, vol. 7, p. 4.
- 13 (a) A. C. Kathalikkattil, K. K. Bisht, N. Aliaga-Alcalde and E. Suresh, *Cryst. Growth Des.*, 2011, **11**, 1631–1641; (b) P.-C. Cheng, P.-T. Kuo, Y.-H. Liao, M.-Y. Xie, W. Hsu and J.-D. Chen, *Cryst. Growth Des.*, 2013, **13**, 623–632; (c) D. Sun, L.-L. Han, S. Yuan, Y.-K. Deng, M.-Z. Xu and D.-F. Sun, *Cryst. Growth Des.*, 2013, **13**, 377–385.
- 14 C.-Q. Wan and T. C. W. Mak, *New J. Chem.*, 2009, **33**, 707–712.
- 15 (a) G. A. Farnum, C. M. Gandolfo, R. M. Supkowski and R. L. LaDuka, *Cryst. Growth Des.*, 2011, **11**, 4860–4875; (b) M. Du, Z.-H. Zhang, C.-P. Li, J. Ribas-Arino, N. Aliaga-Alcalde and J. Ribas, *Inorg. Chem.*, 2011, **50**, 6850–6852; (c) X. He, X.-P. Lu, M.-X. Li and R. E. Morris, *Cryst. Growth Des.*, 2013, **13**, 1649–1654.
- 16 (a) C. S. Campos-Fernández, R. Clérac and K. R. Dunbar, *Angew. Chem., Int. Ed.*, 1999, **38**, 3477–3479; (b) O. S. Jung, Y. J. Kim, Y. A. Lee, K. M. Park and S. S. Lee, *Inorg. Chem.*, 2003, **42**, 844–850; (c) M. R. Sambrook, P. D. Beer, J. A. Wisner, R. L. Paul and A. R. Cowley, *J. Am. Chem. Soc.*, 2004, **126**, 15364–15365; (d) P. Manna, S. K. Seth, A. Das, J. Hemming, R. Prendergast, M. Hellwell, S. R. Choudhury, A. Frontera and S. Mukhopadhyay, *Inorg. Chem.*, 2012, **51**, 3557–3571; (e) P. Wang, L. Luo, T.-A. Okamura, H.-P. Zhou, W.-Y. Sun and Y.-P. Tan, *Polyhedron*, 2012, **44**, 18–27.
- 17 X.-D. Chen and T. C. W. Mak, *Chem. Commun.*, 2005, 3529–3531.
- 18 (a) A. Cingolani, Effendi, M. Pellei, C. Pettinari, C. Santini, B. W. Skelton and A. H. White, *Inorg. Chem.*, 2002, **41**, 6633–6645; (b) N. Lehnert, U. Cornelissen, F. Neese, T. Ono, Y. Noguchi, K. Okamoto and K. Fujisawa, *Inorg. Chem.*, 2007, **46**, 3916–3933; (c) F.-J. Liu, D. Sun, H.-J. Hao, R.-B. Huang and L.-S. Zheng, *Cryst. Growth Des.*, 2012, **12**, 354–361; (d) C. Uyeda and J. C. Peters, *J. Am. Chem. Soc.*, 2013, **135**, 12023–12031.
- 19 (a) M. O. Awaleh, A. Badia and F. Brisse, *Inorg. Chem.*, 2005, **44**, 7833–7845; (b) M. O. Awaleh, A. Badia, F. Brisse and X.-H. Bu, *Inorg. Chem.*, 2006, **45**, 1560–1574; (c) M. O. Awaleh, A. Badia and F. Brisse, *Inorg. Chem.*, 2007, **46**, 3185–3191.
- 20 L. Pauling, *The Nature of the Chemical Bond*, Cornell University Press, Ithaca, NY, 1960, p. 260.
- 21 J. F. Malone, C. M. Murray, M. H. Charlton, R. Docherty and A. J. Lavery, *J. Chem. Soc., Faraday Trans.*, 1997, **93**, 3436.